Molecular Recognition

DOI: 10.1002/ange.200501886

AFM Snapshots of Synthetic Multifunctional Pores with Polyacetylene Blockers: Pseudorotaxanes and Template Effects**

Jiro Kumaki, Eiji Yashima, Guillaume Bollot, Jiri Mareda, Svetlana Litvinchuk, and Stefan Matile**

Synthetic multifunctional pores are constructed from abiotic scaffolds and not only mediate molecular translocation across the membranes of lipid bilayers but also act as hosts or as catalysts.[1,2] Synthetic multifunctional pores became accessible with the discovery of synthetic access to artificial, rigid-rod β barrels. Their practical usefulness as detectors of chemical reactions has been demonstrated,[1,2] and applications toward multicomponent sensing in complex matrixes are in progress.[3] Structural studies naturally have low priority in research focusing on the creation and application of advanced function.[4] Nevertheless, structural studies on molecular recognition by synthetic multifunctional pores under conditions relevant for function indicated that pore blockage occurs by the physical insertion of the guest into the transmembrane host.[4] These findings implied the formation of inclusion complexes with small guests and of pseudorotaxanes[5–11] with macromolecular guests. Herein, we report on atomic force microscopy (AFM) studies in which single polyacetylene-blocked rigid-rod β-barrel pores were imaged as giant, supramacromolecular pseudorotaxanes.

AFM imaging of molecular recognition by synthetic multifunctional pores became a realistic prospect only because of steady progress made in terms of both pores and blockers. The availability of a fine-tuned set of pores covering the complete spectrum of thermodynamic and kinetic stabilities,[12] for example, promised a rapid identification of the optimal characteristics for the self-assembly of barrels on mica during drying from a buffer solution. As in the formation of synthetic multifunctional pores,[12] the unstable but inert, namely, "self-repairing", rigid-rod β-barrel **1** with internal KH dyads and external LLL triads (Figures 1 and 2a) gave the best AFM images rather than stable/inert barrels with internal RH dyads or stable/labile barrels with internal HH dyads.[13] Consistent with previous AFM results,[13] the obtained objects had an average height of approximately 3.6 nm that matched the height of the barrels standing on the mica surface. The heterogeneous height distribution of 2.3–4.1 nm was suggestive of the additional presence of barrels lying sideways on the surface. In this case, barrel widths of up to about 4 nm were conceivable for the "square-type" conformation $\mathbf{1}^{S}$ that was presumed to be observed in single-channel measurements.[12] However, a "diamond-type" conformation $\mathbf{1}^{D}$ could exhibit a barrel width down to about 2 nm. The flattened appearance of vesicles, for example, in tapping-mode AFM images[14] suggests that it was conceivable that external pressure by the AFM tip could compress the square $\mathbf{1}^{S}$ conformation into the local energy minimum of the diamond $\mathbf{1}^{D}$ conformation. Possible stabilization of diamond-like conformations $\mathbf{1}^{D}$ by interactions with the mica surface could neither be excluded nor confirmed.

Previously, anionic polyacetylene blockers such as **2** have served as probes to study molecular recognition by synthetic multifunctional pores in lipid bilayer membranes by circular dichroism (CD) spectroscopy.[15] It now transpires that problems of imaging extended linear polymers on mica with classical blockers such as α-helical or random-coil polyglutamate could also be solved by using the more shape-persistent polyacetylene blockers. Poly(ethyl(4-ethynylphenyl)phosphonate)s **2**[16] were detected as wormlike objects with an average height of 0.66 nm and a local maximal height of 1.1–1.5 nm (Figure 2b). Both values were independent of the molecular-weight distribution, whereas the average length found of course increased from low- to high-molecular-weight polymers.

[*] Dr. J. Kumaki, Prof. E. Yashima
Yashima Super-structured Helix Project, ERATO, JST
Creation Core Nagoya 101, Moriyama-ku
Nagoya 463-0003 (Japan)
Fax: (+81) 52-739-2083
E-mail: kumaki@yp-jst.jp
G. Bollot, Dr. J. Mareda, S. Litvinchuk, Prof. S. Matile
Department of Organic Chemistry
University of Geneva
Geneva, Switzerland
Fax: (+41) 22-379-5123
E-mail: stefan.matile@chiorg.unige.ch

[**] We thank Nathalie Sordé and Duy-Hien Tran for assistance in organic synthesis and the Swiss NSF for financial support (including the National Research Program "Supramolecular Functional Materials" 4047-057496).

Supporting information (experimental details) for this article is available on the WWW under http://www.angewandte.org or from the author.

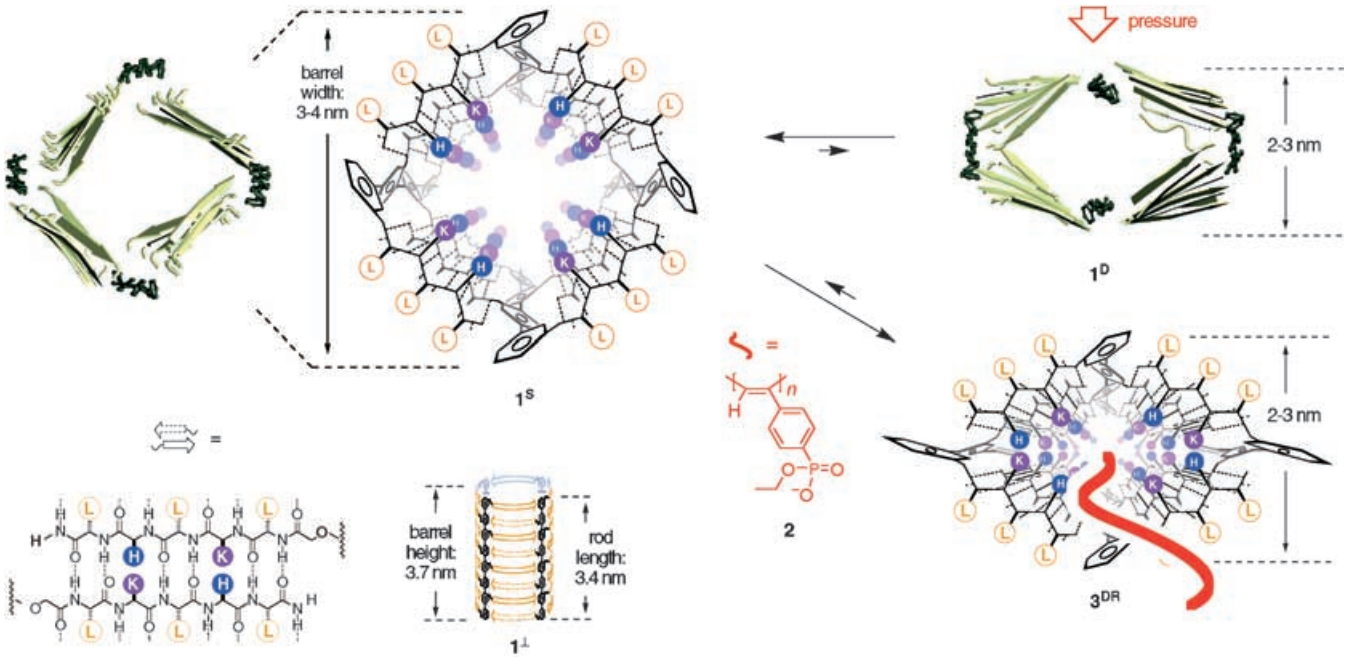

Figure 1. Notional structures and geometry-minimized models of pore **1** in a vertical (⊥) and horizontal position relative to a mica surface in open, "square-like" (**1**^{S}) and closed, "diamond-like" conformations (**1**^{D}) with pseudorotaxane **3**^{DR}, and indication (red) of the expected **S**→**D** contraction by external pressure from the AFM tip and internal templation by blocker **2**.
β Sheets are given as solid (backbone) and dotted lines (hydrogen bonds, **1**^{S}, **1**^{D}, **3**^{DR}) or as arrows (N→C, **1**$^{\perp}$). External amino acid residues are shown in white circles, internal ones in dark circles (single-letter abbreviations).

These characteristics suggested that molecular recognition by synthetic multifunctional pores could be studied by AFM using barrel **1** and polymer **2**. The ability of polymer **2** to block pore **1** in lipid bilayers was confirmed by using methods described previously. The dose/response curve revealed an effective inhibitory concentration (IC_{50}) of 40 nM for a low-molecular-weight polymer **2**. This excellent molecular recognition was confirmed in AFM images of mixtures of pore **1** and blocker **2**. The ratio of bound to free barrels in the above example was 8:1 (Figure 2c); at higher polymer concentrations all the barrels were bound. On average, every second barrel was located at the end of the polymers (Figure 2c, e). Although the probability of observing pseudorotaxane motifs with barrels located more than half of the average polymer length from one terminus should decrease rapidly, the value was still far above the low number of end-on complexes expected for statistical ion pairing along the polymer template (Figure 2e). Under the studied conditions, excluding, for example, the experimentally inaccessible excess barrels, only a few examples with more than one barrel per polymer were found (see, for example, Figure 3, panels d1–d3 and c2).

End-on preference over rotaxane motifs suggested that molecular recognition occurs within the hollow supramolecule and that it is strong enough to hinder the continuing motion of the sticky polymer through the barrel. Consistent with earlier results on blockage and catalysis[12] by synthetic multifunctional pores in bilayer membranes,[4] this result

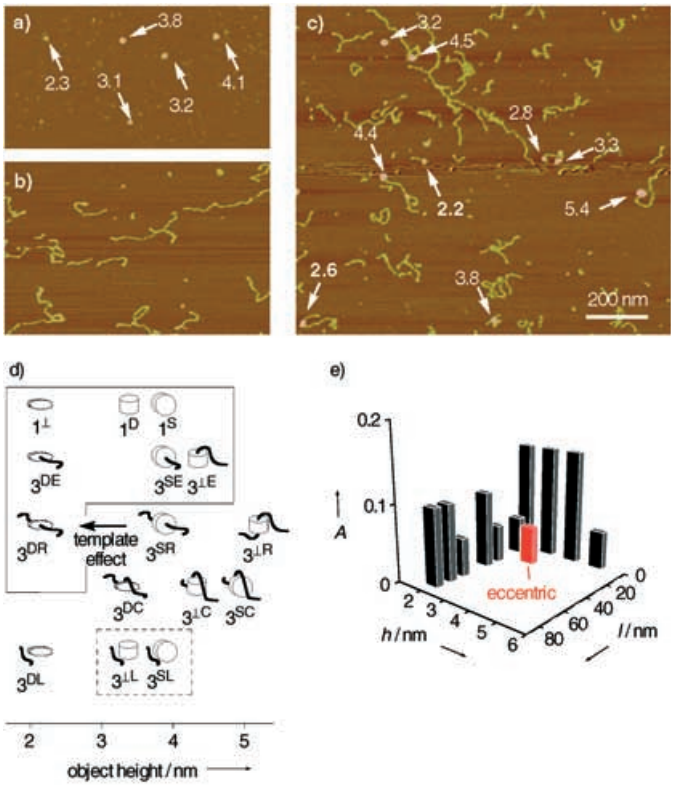

Figure 2. AFM images of a) barrel **1**, b) polymer **2**, and c) **1** and **2** together with object heights indicated in nm. d) Collection of possible structures as a function of their object height. Detected motifs are shown in a solid box, possibly detected in a dotted box, and undetected without a frame. For **1**, **3**, ⊥, **S** (square-like), **D** (diamond-like), and **R** (pseudorotaxane), see Figure 1; **E**: "end-on" complexes, **L**: "lateral" complexes, **C**: crossovers. e) 2D Histogram with the relative abundance *A* as a function of object height *h* and distance *l* from the nearest polymer terminus ($n = 20$); red: eccentric barrel position, see Figure 3e.

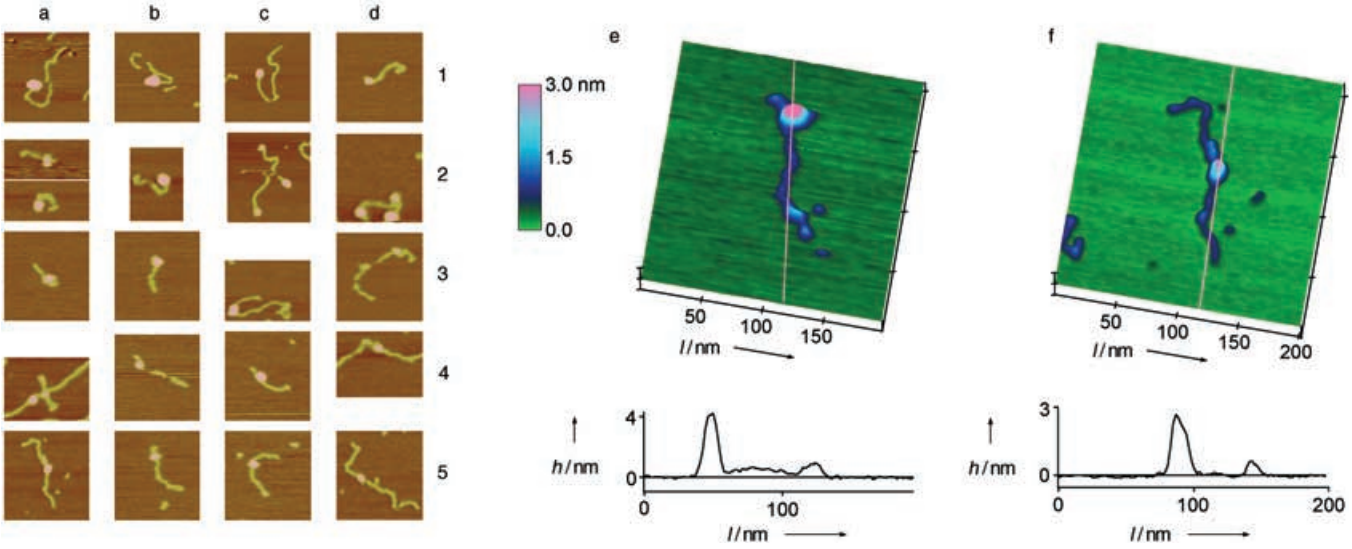

Figure 3. Gallery of rotaxane and "end-on" motifs (a–d, arbitrary scales) with magnification and height profile for eccentric (e) and centered rotaxanes (f).

demonstrated that molecular recognition by synthetic multifunctional pores occurs by threading of the polymer guest through the barrel host to form supramolecular pseudorotaxane complexes $\mathbf{3}^{\mathbf{R}}$. This key finding explained the absence of polyrotaxanes under the studied conditions (namely, more than two barrels per polymer; Figure 3, panels d1–d3 and c2).[5–11] Moreover, it excluded the existence of nonspecific interactions with monomeric rods and at the external barrel surface (that is, lateral complexes $\mathbf{3}^{\mathbf{DL}}$, $\mathbf{3}^{\perp\mathbf{L}}$, and $\mathbf{3}^{\mathbf{SL}}$ as well as crossover motifs $\mathbf{3}^{\mathbf{DC}}$, $\mathbf{3}^{\mathbf{SC}}$, and $\mathbf{3}^{\perp\mathbf{C}}$, Figure 2d).

On average, barrels at the end of the polymer were clearly higher than barrels in the middle (Figure 2c, e). The height distribution of end-on objects $\mathbf{3}^{\mathbf{E}}$ implied that different conformers are likely to exist in different orientations relative to the mica surface (for example, vertical in $\mathbf{3}^{\perp\mathbf{E}}$, horizontal in $\mathbf{3}^{\mathbf{DE}}$, and perhaps the square-type $\mathbf{3}^{\mathbf{SE}}$, Figure 2d). The accumulation of pseudorotaxane motifs with low object height in the middle of the polymer (Figure 2e) excluded the existence of crossover motifs ($\mathbf{3}^{\mathbf{DC}}$, $\mathbf{3}^{\mathbf{SC}}$, $\mathbf{3}^{\perp\mathbf{C}}$) as well as pseudorotaxanes with vertical ($\mathbf{3}^{\perp\mathbf{R}}$) and horizontal barrels in a square-type conformation ($\mathbf{3}^{\mathbf{SR}}$, Figure 2d). Pseudorotaxane $\mathbf{3}^{\mathbf{DR}}$ remained as the only meaningful suprastructure of the frequently found rotaxane-type objects with low height (Figure 2d).

The formation of pseudorotaxane $\mathbf{3}^{\mathbf{DR}}$ suggested that template effects[5–11] may contribute to molecular recognition by synthetic multifunctional pores. Namely, as a polymer guest **2** enters into an open pore $\mathbf{1}^{\mathbf{S}}$, the square-type barrel $\mathbf{1}^{\mathbf{S}}$ may flip into the energetically higher local minimum of the diamond-type barrel $\mathbf{1}^{\mathbf{D}}$ to firmly bite into the internal thread. This experimental evidence for guest templation could, however, not be considered as unambiguous because contributions from the external pressure of the AFM tip to the low barrel width in most rotaxane motifs could not be excluded. However, optimizations of the average geometries obtained during the last 50 ps of a short molecular dynamics simulation revealed the separate local minima of the square- and diamond-shaped conformers of β barrels and of rotaxanes. The conformational change of the square- to diamond-shaped barrel was associated with a pronounced shrinkage of the rod–rod barrel width from 3.5 nm for $\mathbf{1}^{\mathbf{S}}$ to 1.8 nm in the optimized structure of $\mathbf{1}^{\mathbf{D}}$. In the computed structure of the diamond-shaped rotaxane $\mathbf{3}^{\mathbf{DR}}$ (Figure 4), the rod–rod width

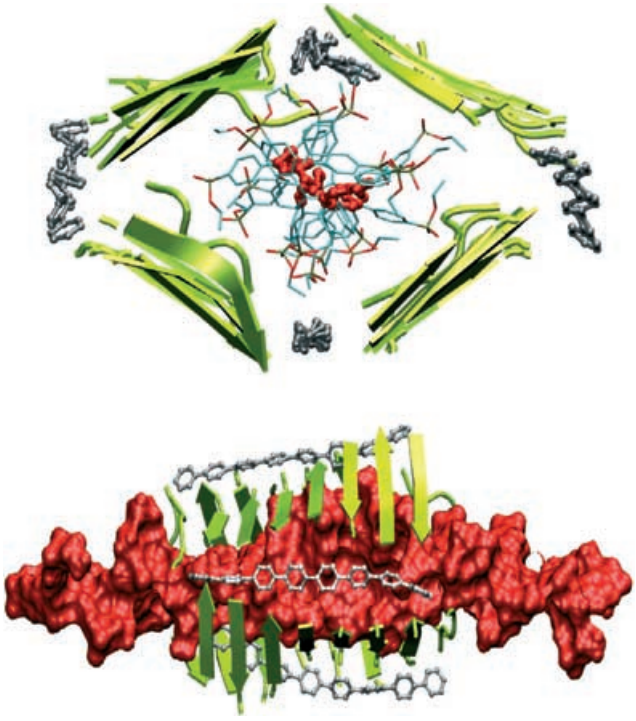

Figure 4. Fully optimized cutaway structures of diamond-shaped pseudorotaxane $\mathbf{3}^{\mathbf{DR}}$ in axial view (top, **2**: 20-mer, backbone in red) and in side view (bottom: **2**: 40-mer, Connolly surface in red). β Sheets are highlighted as arrows (green), *p*-octaphenyl groups as ball-and-stick models (silver); 100% phosphonate deprotonation, 100% K and 0% H protonation.

was also reduced to 2.2 nm. This finding corroborated the proposal of guest templation and was in agreement with the nonstatistical height distribution in the AFM images (Figure 2e). Similar guest templation has been observed in previous molecular dynamics simulations with α-helical blockers.[4]

The few rotaxane motifs observed with object heights exceeding the range of 2–3 nm expected for diamond-type pseudorotaxanes $\mathbf{3}^{\mathbf{DR}}$ could not be interpreted convincingly (Figure 2e). The eccentric position of the barrel with respect to the polymer was consistent with lateral complexes $\mathbf{3}^{\perp\mathbf{L}}$ or $\mathbf{3}^{\mathbf{SL}}$ (Figures 2d, 3e). The existence of nonspecific surface-to-surface association was, however, incompatible with the observed nonstatistical location of the barrel on the polymer. These infrequent rotaxane motifs with eccentric and high barrels may, therefore, be considered either as diamond-type pseudorotaxanes $\mathbf{3}^{\mathbf{DR}}$ with imperfect barrel positioning or as an "accidental" detection of unfavored lateral complexes $\mathbf{3}^{\perp\mathbf{L}}$/$\mathbf{3}^{\mathbf{SL}}$ at the single-molecule level without relevance to the average of the ensemble. The interpretation and significance of this exception—but not of the more important and unambiguous end-on preference and low-height pseudorotaxanes—deserve further reservation considering the low number of complexes observed as well as unexplored alternative conditions.

In summary, AFM snapshots of molecular recognition by synthetic multifunctional pores provide experimental evidence that the host–guest complexes formed between rigid-rod β-barrel pore and polymer blockers are pseudorotaxanes. The nonstatistical location of the barrel on the polymer indicates that entry of the polymer into the pore is favored over the motion of the polymer through the sticky pore. Although the clearly different conditions call for cautious interpretation,[4] it can be considered as structural support for the possibility of blocker efflux through blocked, "blocker-selective" pores, a concept central to the understanding of synthetic multifunctional pores that has been verified previously at the functional level.[17] Predicted[4] and supported in silico, the nonstatistical object height distribution can be considered, with similar caution, as the so far elusive structural evidence for guest templation during molecular recognition by synthetic multifunctional pores.

Received: May 31, 2005
Published online: August 26, 2005

Keywords: bioorganic chemistry · ion channels · molecular recognition · scanning probe microscopy · supramolecular chemistry

[1] N. Sakai, J. Mareda, S. Matile, *Acc. Chem. Res.* **2005**, *38*, 79–87.
[2] N. Sakai, S. Matile, *Chem. Commun.* **2003**, 2514–2523.
[3] S. Litvinchuk, N. Sordé, S. Matile, *J. Am. Chem. Soc.* **2005**, *127*, 9316—9317.
[4] Y. Baudry, G. Bollot, V. Gorteau, S. Litvinchuk, J. Mareda, M. Nishihara, D. Pasini, F. Perret, D. Ronan, N. Sakai, M. R. Shah, A. Som, N. Sordé, P. Talukdar, D.-H. Tran, S. Matile, *Adv. Funct. Mater.*, in press.
[5] *Molecular Catenanes, Rotaxanes and Knots* (Eds.: J.-P. Sauvage, C. Dietrich-Buchecker), Wiley-VCH, Weinheim, **1999**.
[6] A. Harada, *Acc. Chem. Res.* **2001**, *34*, 456–464.
[7] V. Balzani, A. Credi, F. M. Raymo, J. F. Stoddart, *Angew. Chem.* **2000**, *112*, 3484–3530; *Angew. Chem. Int. Ed.* **2000**, *39*, 3348–3391.
[8] J. K. M. Sanders, *Pure Appl. Chem.* **2000**, *72*, 2265–2274;
[9] O. Lukin, F. Vögtle, *Angew. Chem.* **2005**, *117*, 1480–1501; *Angew. Chem. Int. Ed.* **2005**, *44*, 1456–1477.
[10] A. M. Brouwer, C. Frochot, F. G. Gatti, D. A. Leigh, L. Mottier, F. Paolucci, S. Roffia, G. W. H. Wurpel, *Science* **2001**, *291*, 2124–2128.
[11] J. W. Lee, S. Samal, N. Selvapalam, H.-J. Kim, K. Kim, *Acc. Chem. Res.* **2003**, *36*, 621–630.
[12] S. Litvinchuk, G. Bollot, J. Mareda, A. Som, D. Ronan, M. R. Shah, P. Perrottet, N. Sakai, S. Matile, *J. Am. Chem. Soc.* **2004**, *126*, 10067–10075.
[13] G. Das, L. Ouali, M. Adrian, B. Baumeister, K. J. Wilkinson, S. Matile, *Angew. Chem.* **2001**, *113*, 4793–4797; *Angew. Chem. Int. Ed.* **2001**, *40*, 4657–4661.
[14] Y. Tanaka, M. Miyachi, Y. Kobuke, *Angew. Chem.* **1999**, *111*, 565–567; *Angew. Chem. Int. Ed.* **1999**, *38*, 504–506.
[15] G. Das, H. Onouchi, E. Yashima, N. Sakai, S. Matile, *ChemBioChem* **2002**, *3*, 1089–1096.
[16] H. Onouchi, D. Kashiwagi, K. Hayashi, K. Maeda, E. Yashima, *Macromolecules* **2004**, *37*, 5495–5503.
[17] D. Ronan, N. Sordé, S. Matile, *J. Phys. Org. Chem.* **2004**, *17*, 978–982.

